Available online at www.sciencedirect.com

ScienceDirect

Ceramics International 35 (2009) 433–439

CERAMICS INTERNATIONAL

www.elsevier.com/locate/ceramint

Effect of M-doping (M = Fe, V) on the photocatalytic activity of nanorod rutile TiO_2 for Congo red degradation under the sunlight

Khaled Melghit[a,*], Odheiba S. Al-Shukeili[a], Issa Al-Amri[b]

[a] *Chemistry Department, College of Science, Sultane Qaboos University, P.O. Box 36, Al Khodh 123, Oman*
[b] *Electron Microscopy Unit, College of Medicine and Health Sciences, Sultane Qaboos University, P.O. Box 36, Al Khodh 123, Oman*

Received 25 September 2007; received in revised form 20 October 2007; accepted 3 December 2007

Abstract

Nanorods TiO_2, Fe-TiO_2 (3 and 2 at.% Fe), V-TiO_2 (5 at.% V) were prepared by a low temperature method and characterized by powder X-ray diffraction, thermal analysis, transmission electron microscope and BTE surface area analysis. The as-prepared samples were evaluated as catalysts for photodegradation of Congo red aqueous solution under the sunlight. Nanorods Fe-doped TiO_2 shows higher adsorption and also higher photocatalytic degradation of Congo red solution compared to pure nanorods TiO_2 rutile. A higher activity is obtained when the amount of doped Fe is 2 at.%, compared to 3 at.%. However, nanorods V-TiO_2 does not show neither adsorption nor photodegradation activity of Congo red solution.

Keywords: Photodegradation; Congo red; Fe-doped TiO_2; V-doped TiO_2

1. Introduction

Titanium oxide TiO_2 is widely used for photodegradation of many organic toxic compounds [1–7]. Anatase and rutile are the common TiO_2 structures used. In general, UV energy is used to initiate the photocatalytic reaction. This energy allows transition of electron from TiO_2 valence band to conducting band. At the present time, many researches are carried out in order to substitute the UV light by the sunlight or visible light. This will reduce the cost of the photodegradation process especially for industrial scale applications. Using dopants that can be incorporated in TiO_2 lattice is one of the methods used to reach this goal [8–18]. Results show that doping TiO_2 with transition metals increases its photocatalytic activity [11–18]. It is reported that doped ions can enhance the intensity of absorption in the UV–vis light region and make a red shift in the band gap transition of the doped TiO_2 samples. For example in the case of Fe-TiO_2 sample, Fe^{3+} ions can have two roles: they can act as a photo-generated hole and a photo-generated electron trap and reduce the hole–electron recombination and also they can serve as a mediator of the transfer of interfacial charge [15,19]. However, there is a controversy on the effect of metals ions on the photocatalytic activity of TiO_2. Other authors show a decrease of photocatalytic activity of the doped catalysts [20–23]. The amount of the metal ions that can be incorporated in TiO_2 lattice is also a controversial matter [15,17,18].

Recently we show that nanorods of titanium oxide rutile present good photocatalytic activity for Congo red degradation under the sunlight [24]. The present paper investigates the effect of doping by iron and vanadium on nanorods TiO_2 rutile for Congo red degradation under the sunlight.

2. Experimental

2.1. TiO_2

In this preparation, similar method recently published [24] was used. About 5 mL of $TiCl_3$ (30% (w/v), DBH Chemical Ltd., Poole England) was diluted with 45 mL of distilled water and stirred for about 65 h at room temperature. The dark purple color of the solution turned to white colloidal solution with pH 0.8. Then, 500 mL of distilled water was added followed by about 20 mL of 10% NH_4OH. The pH of the solution became basic ~9 and a white gel appeared. The gel at the bottom of the beaker was easily separated from the solution by decantation. Then, it was washed with distilled water several times until the

---

* Corresponding author. Tel.: +968 24142449; fax: +968 24413415.
E-mail address: melghit@squ.edu.om (K. Melghit).

0272-8842/$34.00
doi:10.1016/j.ceramint.2007.12.009

$AgNO_3$ test indicates absence of chloride ion Cl^- in the solution. The wet gel obtained was dried at room temperature.

2.2. *Fe-doped TiO_2*

Similar to the method recently reported [25]. The wet TiO_2 gel obtained as described above was heated until boiling. At the same time $Fe(NO_3)_3{\cdot}9H_2O$ (DBH Chemical Ltd., Poole England) was dissolved in 100 mL of distilled water and heated until boiling. The starting molar ratio used was Ti/Fe: 16/1. The iron solution was mixed to the wet TiO_2 gel and stirred for 15 min at ~100 °C. The product obtained was washed with distilled water several times and dried at room temperature.

2.3. *V-doped TiO_2*

Similar to preparation of Fe-TiO_2; the wet gel TiO_2 was heated until boiling. At the same time, a solution of vanadium oxide was prepared according to the method recently published [26] [0.250 g of V_2O_5 (BDH Chemicals Ltd., Poole England) was dissolved in 3 mL of H_2O_2 (30%, w/v) and stirred for about 4 min. Then, 400 mL of distilled water was added and the mixture was heated until boiling]. The starting molar ratio used was Ti/V: 6/1. The vanadium solution was mixed to the wet TiO_2 gel and stirred for 15 min at ~100 °C. The product obtained was dried at room temperature.

Congo red is water soluble; yielding a red solution with absorption bonds in UV–vis spectrum located around 340 and 500 nm. It has the following chemical structure:

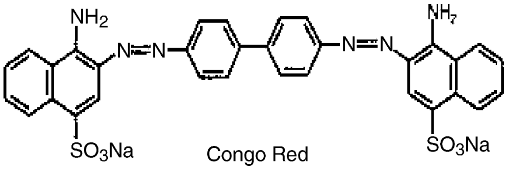

The Congo red solution was prepared by dissolving Congo red powder ($C_{32}H_{24}N_6O_6S_2$ from BDH Chemical Ltd., Poole England) in distilled water to obtain a solution 2.5×10^{-5} M concentration. The photocatalysis experiments were carried out in 100 mL beaker containing about 80 mL of 0.025 mM of Congo red aqueous solution and about 0.100 g of catalyst. The mixtures were stirred about 15 min in the dark, then the solutions were exposed to the sunlight for about 35 min with continuous stirring between 11:00 a.m. and 12:00 p.m. the intensity of the sunlight, during photodegradation experiment was measured by a Radiometer (model PMA2100, Solar Light Company, Inc.). Catalysts and solutions were characterized by different spectroscopic techniques as powder X-ray diffraction (Philips 1710, diffractometer), thermal analysis (TG and DTA, 2960 Universal TA Instruments, under nitrogen gas and with heating rate 10 °C min^{-1}), UV–vis spectroscopy (UV spectrometer Cary 50 Conc) and transmission electron microscope (Jeol 1234). The elemental analysis was measured by an Oxford EDAX detector connected to JEOL JSM-840A scanning electron microscope. The surface area of the catalysts were determined with standard BET apparatus (Autosorb-1, Quantachrome).

3. Results and discussion

Fig. 1 shows the X-ray diffraction pattern of the three as-prepared samples (a) TiO_2, (b) Fe-TiO_2 and (c) V-TiO_2; all phases show similar diffraction peaks that can be indexed with rutile lattice. Doped TiO_2 phases (Fe-TiO_2 and V-TiO_2) do not show any diffraction peaks of iron or vanadium or related compounds. Although, if the impurity amount is low; it can be out off the detection limit of the X-ray diffractometer. Also because the products are obtained by a low temperature method (100 °C), it is possible that some amount of amorphous impurity phase exists which will crystallize and appear at high temperature. Fig. 2 shows the as-prepared samples (TiO_2, Fe-TiO_2 and V-TiO_2) heated at 650 °C for 5 h; the X-ray diffraction peaks become narrow which probably is the consequence of particles size growing. All peaks present in the three phases can be indexed with the rutile lattice. No extra peaks can be seen

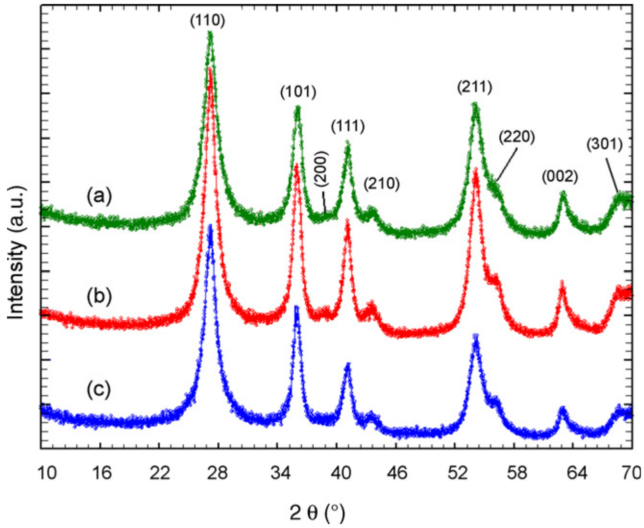

Fig. 1. Powder X-ray diffraction patterns of: (a) TiO_2, (b) Fe-TiO_2 and (c) V-TiO_2.

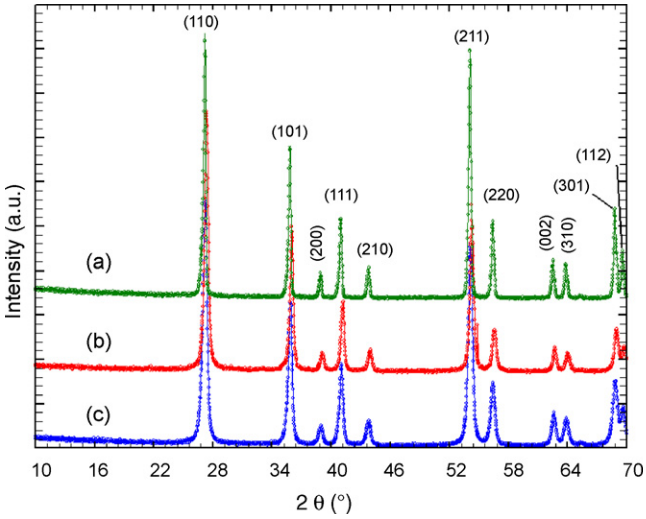

Fig. 2. Powder X-ray diffraction patterns of: (a) V-TiO_2, (b) Fe-TiO_2 and (c) TiO_2 heated at 650 °C for 5 h.

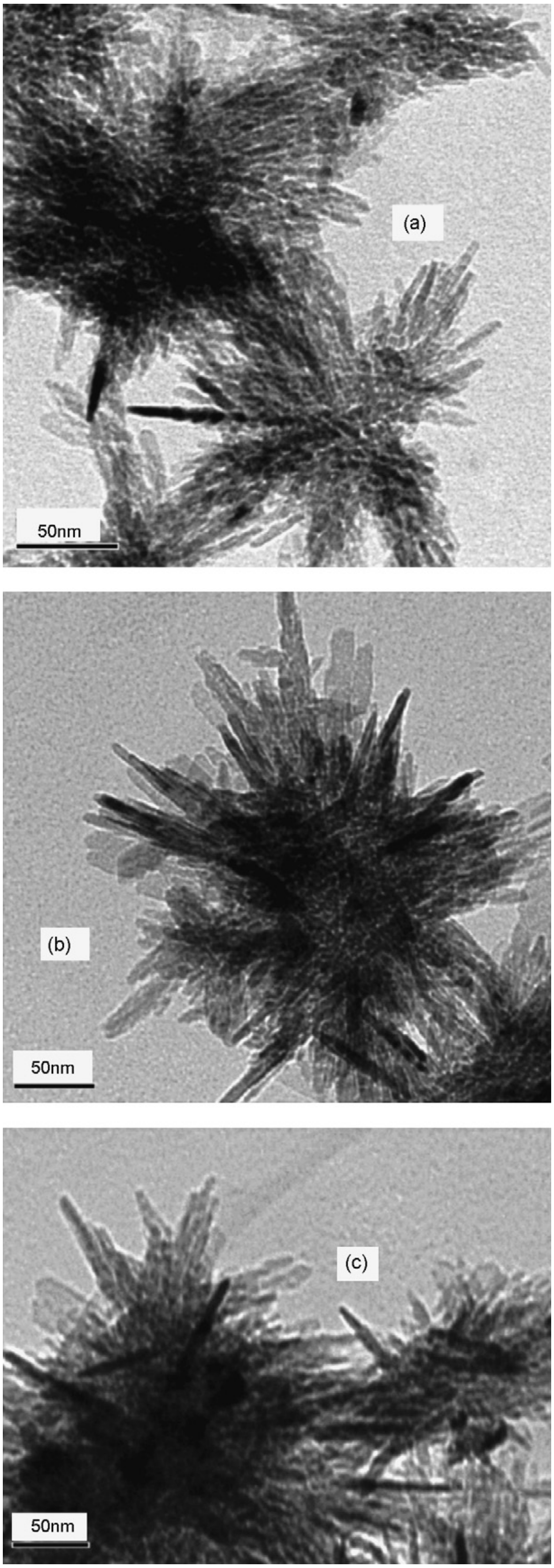

Fig. 3. TEM micrographs of as-prepared samples: (a) TiO_2, (b) Fe-TiO_2 and (c) V-TiO_2.

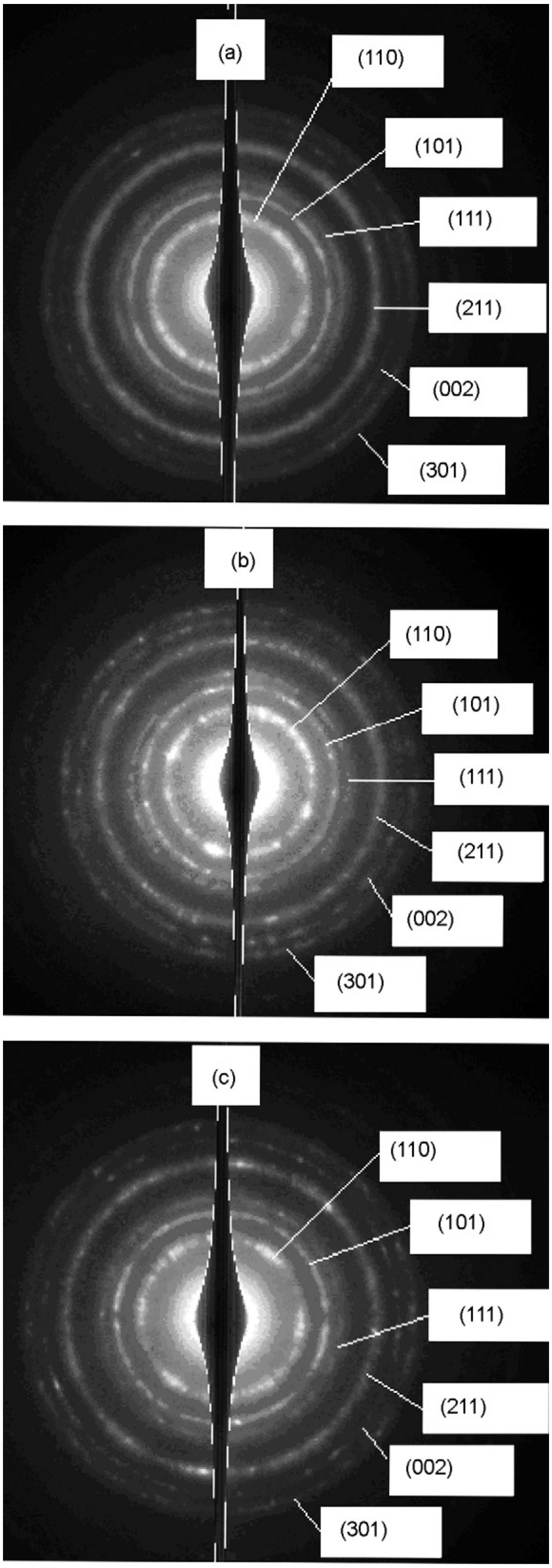

Fig. 4. Selected area electron diffraction patterns of as-prepared: (a) TiO_2, (b) Fe-TiO_2 and (c) V-TiO_2.

Table 1
The surface area of as-prepared powders

Molecular formula	Surface area (m^2/g)
$TiO_2{\cdot}2.8H_2O$	159
$Fe_{0.03}Ti_{0.97}O_{2-\delta}{\cdot}1.0H_2O$	240
$V_{0.05}Ti_{0.95}O_{2+\delta}{\cdot}1.9H_2O$	201

which indicate the absence of any amorphous phase with the three samples. This indicated that the as-prepared phases are crystallized without any other amorphous impurity phase. TEM micrographs (Fig. 3) show that the three samples have almost similar nanorod shape and size. Selected area electron diffraction for the three samples (Fig. 4) show presence only of rutile spotty ring without additional diffraction spots and rings of Fe or V or any related compounds. EDAX analyses show presence of 3 at.% Fe in the Fe-doped TiO_2 and about 5 at.% V for V-doped TiO_2. These two elements are incorporated in rutile TiO_2 lattice. The surface areas of the three as-prepared samples were measured. It increases with doping (Table 1). This result was also observed in recent reported study [14]. The Fe-TiO_2 shows higher surface area than V-TiO_2. TGA curve of as-prepared TiO_2 (Fig. 5) shows that the sample lost its water in three steps. DTA curves shows three endothermic peaks at 93, 164 and 296 °C; the first endothermic peak corresponds to the lost of adsorbed water while the two other peaks correspond to the lost of chemically bonded water. The dehydration process can be summarized as follows:

$$TiO_2 \cdot 2.8H_2O \xrightarrow{143\,^{\circ}C} TiO_2 \cdot 1.2H_2O \xrightarrow{264\,^{\circ}C} TiO_2 \cdot 0.2H_2O \xrightarrow{400\,^{\circ}C} TiO_2$$

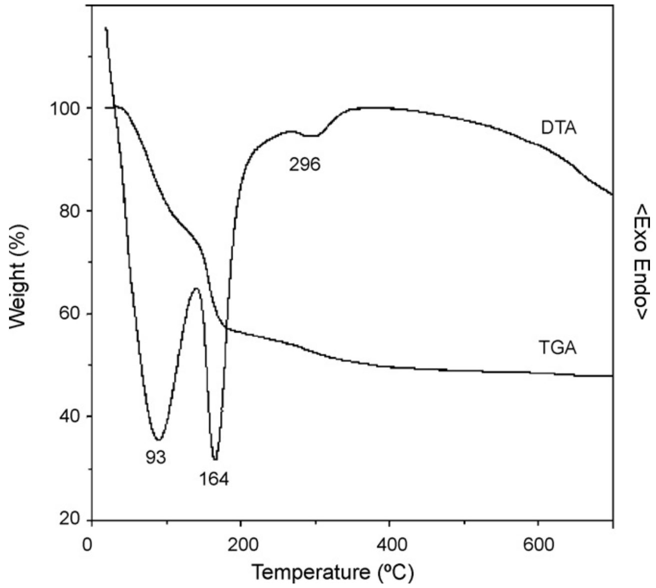

Fig. 5. TGA and DTA of as-prepared TiO_2.

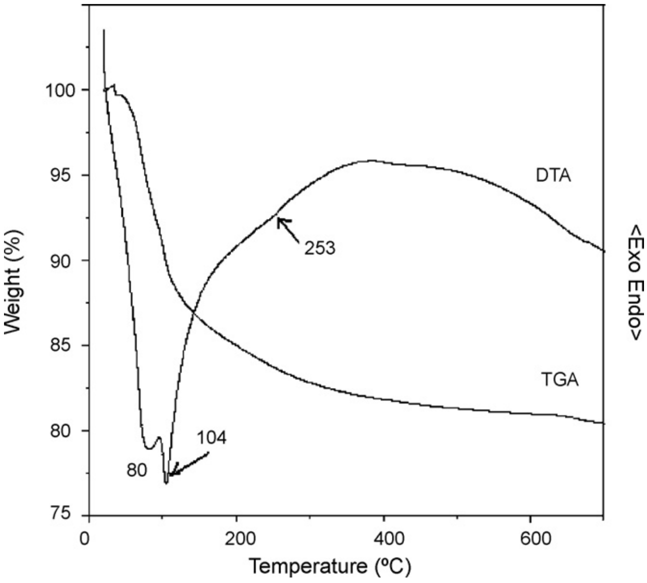

Fig. 6. TGA and DTA of as-prepared Fe-TiO_2.

Fe-TiO_2 lost its water in three steps (Fig. 6), DTA curves shows three endothermic peaks: two intense peaks at 80 and 104 °C, and small broad peak at 253 °C. The two first endothermic peaks correspond to the lost of adsorbed water while the third peak corresponds to the lost of chemically bonded water. TG curve shows a slow and continuous weight loss up to 650 °C. The dehydration process can be summarized as follows:

$$Fe\text{-}TiO_2 \cdot 1.0H_2O \xrightarrow{116\,^{\circ}C} Fe\text{-}TiO_2 \cdot 0.4H_2O \xrightarrow{300\,^{\circ}C} Fe\text{-}TiO_2 \cdot 0.1H_2O \xrightarrow{650\,^{\circ}C} Fe\text{-}TiO_2$$

Also V-TiO_2 lost its water on three steps (Fig. 7), DTA curve shows three endothermic peaks: one intense peak at 78 °C, and two small broad peaks at 162 and 321 °C. The first endothermic peak corresponds to the lost of adsorbed water while the second and third peaks correspond to the lost of chemically bonded

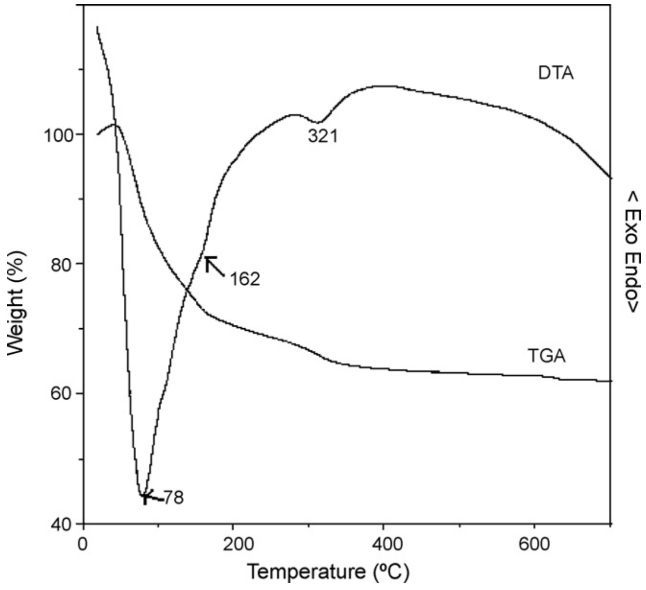

Fig. 7. TGA and DTA of as-prepared V-TiO_2.

Table 2
Unit cell parameters and volume of as-prepared samples (calculations carried out using Dicvol04 program [27])

	$TiO_2{\cdot}2.8H_2O$	$V_{0.05}Ti_{0.95}O_{2+\delta}{\cdot}1.9H_2O$	$Fe_{0.03}Ti_{0.97}O_{2-\delta}{\cdot}1.0H_2O$
a (Å)	4.6161	4.6121	4.6230
c (Å)	2.9508	2.9483	2.9536
V (Å^3)	62.88	62.72	63.12

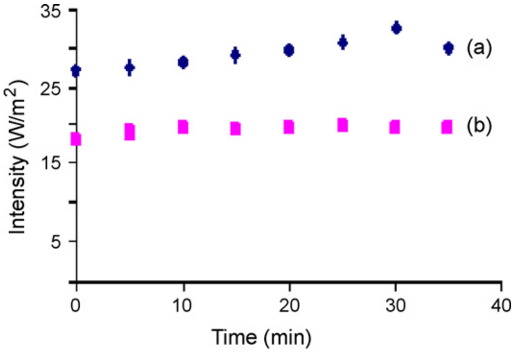

Fig. 9. Solar intensity variation (a) experiment using TiO_2, Fe-TiO_2, V-TiO_2 as catalysts and (b) experiment using 2 at.% Fe-TiO_2 and 3 at.% Fe-TiO_2 as catalysts.

water. The dehydration process can be summarized as follows:

$$\text{V-TiO}_2\cdot 1.9\text{H}_2\text{O}\xrightarrow{96\,^\circ\text{C}}\text{V-TiO}_2\cdot 0.95\text{H}_2\text{O}\xrightarrow{223\,^\circ\text{C}}\text{V-TiO}_2\cdot 0.3\text{H}_2\text{O}\xrightarrow{370\,^\circ\text{C}}\text{V-TiO}_2$$

In general, crystallization of an amorphous phase is an exothermic process that will appear on the DTA curve as an exothermic peak. The as-prepared three samples show absence of exothermic peaks on the DTA curves which confirm the absence of any amorphous phase. This is consistent with the X-ray diffraction patterns of the as-prepared samples heated at 650 °C (Fig. 2). The as-prepared samples will correspond to the following formula: $TiO_2{\cdot}2.8H_2O$, $Fe_{0.03}Ti_{0.97}O_{2-\delta}{\cdot}1.0H_2O$ and $V_{0.05}Ti_{0.95}O_{2+\delta}{\cdot}1.9H_2O$. The above analyses confirm the high level of purity of the three phases obtained. Using Dicvol04 program [27], calculation of the unit cell parameters and volume were performed on the as-prepared samples (Table 2). The V-doped TiO_2 shows small decrease in the unit cell parameters, however Fe-doped TiO_2 shows a small increase which are consistent with their ionic radius values [28]: V^{5+} (0.540 Å), Fe^{3+} (0.645 Å) compared to Ti^{4+} (0.605 Å) ions. The increase of unit cell parameters, for Fe-doped TiO_2, was also recently reported in Fe-doped TiO_2 anatase [29,30]. This may indicate that the Fe^{3+} and V^{5+} ions have been incorporated into the rutile lattice. The three samples were evaluated as catalyst for Congo red degradation. To compare their adsorption, they are first mixed with Congo red solution and stirred for 15 min in the dark. The UV spectra are shown in Fig. 8. The adsorption of Fe-TiO_2 was found to be better than the parent sample TiO_2. Probably, because of the high surface area obtained with Fe-TiO_2 compared to TiO_2. However the Congo red adsorption did not take place with V-TiO_2 sample, although its surface area is higher than TiO_2. Its UV spectrum shows higher absorbance at 500 nm and much higher around 340 nm. This indicated that the reaction of Congo red with V-TiO_2 surface is different compared to Fe-TiO_2 and TiO_2. The same experiments were carried out, this time, under the sunlight for 35 min. The sunlight intensity, on the period of the experiment, was almost constant without significant change (Fig. 9a). Fig. 10 shows the UV spectra results. Better Congo red degradation was obtained with Fe-TiO_2 than the parent sample TiO_2; this is consistent with published results [11–18]. The UV spectrum of Congo red solution catalyzed with V-TiO_2 under the sunlight is different from the other two catalysts. The peak at 500 nm has higher absorbance compared to the one of Congo red solution, even higher than the value obtained when the experiment was carried out in the dark. For the peak around 340 nm, it becomes broader with higher absorbance. It seems that V-TiO_2 catalyzed a reaction which leads probably to a different compound. In order to study the effect of the amount of iron doped on TiO_2 for Congo red degradation; a similar preparation, as described above, was carried out with less amount of iron. The initial molar ratio was Ti/Fe: 16/0.32. EDAX analysis shows 2 at.%

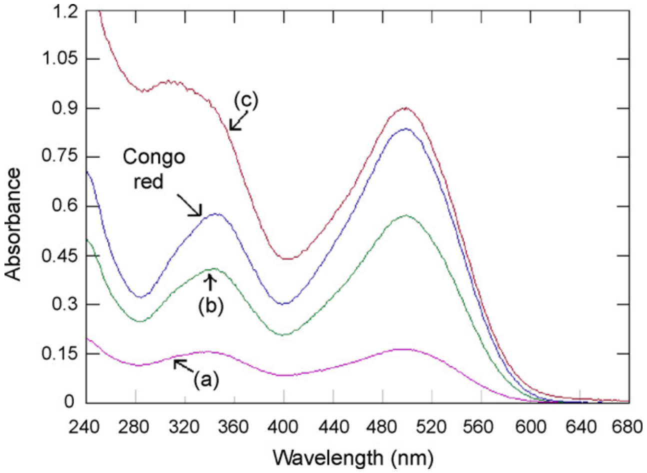

Fig. 8. UV spectra of Congo red solution after separation from the catalyst, with (a) Fe-TiO_2, (b) TiO_2 and (c) V-TiO_2, stirred in dark for 15 min.

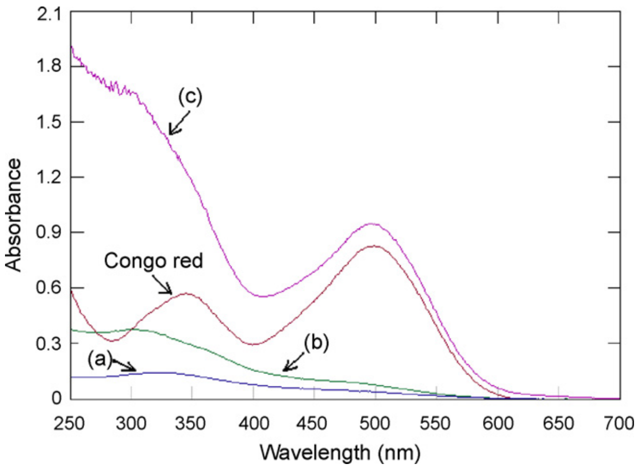

Fig. 10. UV spectra of Congo red solution after separation from the catalyst, with (a) Fe-TiO_2, (b) TiO_2 and (c) V-TiO_2, stirred under sunlight for 35 min.

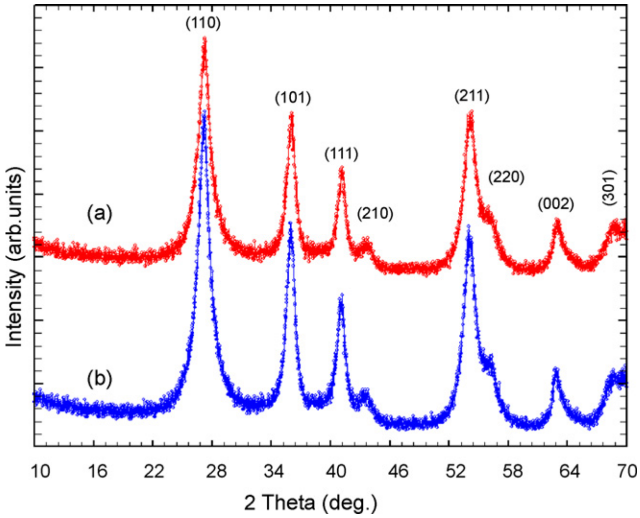

Fig. 11. Powder X-ray diffraction patterns (a) 3 at.% Fe-TiO_2 and (b) 2 at.% Fe-TiO_2.

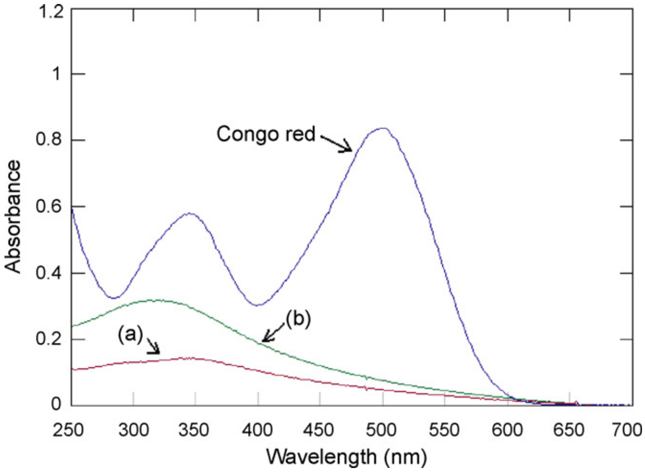

Fig. 12. UV spectra of Congo red solution after separation from the catalyst, with (a) 2 at.% Fe-TiO_2 and (b) 3 at.% Fe-TiO_2, stirred under sunlight for 35 min.

Fe. Fig. 11 shows the X-ray diffraction patterns of both as-prepared samples 3 and 2 at.% Fe. They show similar crystalline phase. For both samples, similar photocatalytic experiments were carried out under the sunlight for 35 min. The sunlight intensity on the period of the experiment was almost constant without significant change, however with less intensity compared to the previous experiment (Fig. 9b). The UV spectra (Fig. 12) shows better photocatalytic activity for the Congo red degradation when the amount of Fe is lowered which is consistent with the reported results [15]. Considering the Fe-doped TiO_2 which presents higher photocatalytic activity, the behavior of V-TiO_2, in the present work, was unexpected. It is worthnoting that methylene blue solution shows degradation over V-TiO_2 (rutile) [14]. It seems that many parameters can interfere on the photocatalytic process of the metal-doped titanium oxide (M-TiO_2). Some of these parameters are: the nature of the metal ions, the crystalline structure of TiO_2, the shape and size of TiO_2 particles, and the pollutant nature. It appears difficult to generalize the result obtain with one system M-TiO_2 with specific characteristic and particular pollutant solution to the other systems with different experimental parameters. All these show the complexity of the system M-TiO_2 catalyst and explain the controversies between authors.

4. Conclusion

Doping titanium oxide nanorods with metals ions can enhance its photocatalytic activity however it is not always the case. While, iron-doped TiO_2 shows higher photocatalytic activity compared to pure TiO_2 for Congo red degradation. Vanadium-doped TiO_2 was found to be inactive. Because the photocatalytic reaction of doped TiO_2 depends on many experimental parameters, it seems to be difficult to expect the photocatalytic activity behavior of M-TiO_2 systems without experimental testing.

Acknowledgements

We thank Sultan Qaboos University for financial support (IG/SCI/CHEM/06/01). Also we thank Mr. Nasser Al-Mandhary for TGA and DTA measurements and Samira Al-Kharousi for XRD measurements.

References

[1] R.J. Gonzalez, R. Zallen, H. Berger, Phys. Rev. B 55 (1997) 7014.
[2] A. Pottier, C. Chance, E. Tronc, L. Mazerroles, J. Jolivet, J. Mater. Chem. 11 (2001) 1116.
[3] H. Lachheb, E. Puzenat, A. Houas, M. Ksibi, E. Elaloui, C. Guillard, J.M. Hermann, Appl. Catal. B: Environ. 39 (2002) 75.
[4] A. Hagfeldt, M. Gratzel, Chem. Rev. 95 (1995) 49.
[5] H. Yamashita, Y. Ichihashi, M. Harada, G. Stewart, M.A. Fox, M. Anpo, J. Catal. 158 (1996) 97.
[6] A.L. Linsebigler, G. Lu, J.T. Yates, Chem. Rev. 95 (1995) 735.
[7] A. Fujishima, T.N. Rao, D.A. Tryk, J. Photochem. Photobiol. C 1 (2000) 1.
[8] W. Choi, A. Termin, M.R. Hoffmann, J. Phys. Chem. 98 (1994) 13669.
[9] R. Asahi, T. Morikawa, T. Ohwaki, K. Aoki, Y. Taga, Science 293 (2001) 269.
[10] A.R. Gandhe, J.B. Fernandes, J. Solid. State. Chem. 178 (2005) 2953.
[11] W. Choi, A. Termin, M.R. Hoffman, Angew. Chem. Int. 33 (1994) 1091.
[12] D. Chatterjee, S. Dasguple, J. Photochem. Photobiol. C: Rev. 6 (2005) 185.
[13] D. Masih, H. Yoshitake, Y. Izumi, Appl. Catal. A: Gen. 325 (2007) 276.
[14] M.M. Mohamed, M.M. Al-Esaimi, J. Mol. Catal. A: Chem. 255 (2006) 53.
[15] M. Zhou, J. Yu, B. Cheng, J. Hazard. Mater. B 137 (2006) 1838.
[16] J.C.-S. Wu, C.-H. Chen, J. Photochem. Photobiol. A: Chem. 163 (2004) 509.
[17] A. Kubacka, A. Fuerte, A. M-Arias, M. F-Garcia, Appl. Catal. B: Environ. 74 (2007) 26.
[18] J. Zhou, M. Takeuchi, A.K. Ray, M. Anpo, X.S. Zhao, J. Colloid Interface Sci. 311 (2007) 497.
[19] T. Ohno, T. Tsubota, M. Toyofuku, R. Inaba, Catal. Lett. 98 (2004) 255.
[20] D.W. Bahnemann, S.N. Kholuiskaya, R. Dillert, A.I. Kulak, A.I. Kokorin, Appl. Catal. B. Environ. 36 (2002) 161.
[21] K. Nagaveni, M.S. Hegde, G. Madras, J. Phys. Chem. B 108 (2004) 20204.
[22] N. San, A. Hatipoglu, G. Kocturk, Z. Cmar, J. Photochem. Photobiol. A: Chem. 146 (2002) 189.
[23] U. Siemon, D. Bahnemann, J.J. Testa, D. Rodriguez, M.I. Litter, N. Bruno, J. Photochem. Photobiol. A: Chem. 148 (2002) 247.

[24] K. Melghit, S.S. Al-Rabaniah, J. Photochem. Photobiol. A: Chem. 184 (2006) 331.
[25] K. Melghit, K. Bouziane, J. Alloys Compd. 453 (2008) 102.
[26] K. Melghit, A.K. Al-Belushi, I. Al-Amri, Ceram. Int. 33 (2007) 285.
[27] A. Boultif, D. Louer, J. Appl. Cryst. 37 (2004) 724.
[28] R.D. Shannon, Acta Crystallogr. A 32 (1976) 751.
[29] K. Melghit, K. Bouziane, J. Am. Ceram. Soc. 90 (7) (2007) 2113.
[30] J. Yang, M. Sen, S. Quaresma, P. Norby, J.M.F. Ferreira, Acta Mater. 53 (2005) 1479.